Environ. Res. Lett. **6** (2011) 034032 (8pp) doi:10.1088/1748-9326/6/3/034032

Climate forcing and response to idealized changes in surface latent and sensible heat

George A Ban-Weiss[1,3], Govindasamy Bala[2], Long Cao[1], Julia Pongratz[1] and Ken Caldeira[1]

[1] Department of Global Ecology, Carnegie Institution, 260 Panama Street, Stanford, CA 94305, USA
[2] Divecha Center for Climate Change and Center for Atmospheric and Ocean Sciences, Indian Institute of Science, Bangalore-560 012, India

E-mail: kcaldeira@carnegie.stanford.edu

Received 20 May 2011
Accepted for publication 24 August 2011
Published 14 September 2011
Online at stacks.iop.org/ERL/6/034032

Abstract
Land use and land cover changes affect the partitioning of latent and sensible heat, which impacts the broader climate system. Increased latent heat flux to the atmosphere has a local cooling influence known as 'evaporative cooling', but this energy will be released back to the atmosphere wherever the water condenses. However, the extent to which local evaporative cooling provides a global cooling influence has not been well characterized. Here, we perform a highly idealized set of climate model simulations aimed at understanding the effects that changes in the balance between surface sensible and latent heating have on the global climate system. We find that globally adding a uniform 1 W m^{-2} source of latent heat flux along with a uniform 1 W m^{-2} sink of sensible heat leads to a decrease in global mean surface air temperature of 0.54 ± 0.04 K. This occurs largely as a consequence of planetary albedo increases associated with an increase in low elevation cloudiness caused by increased evaporation. Thus, our model results indicate that, on average, when latent heating replaces sensible heating, global, and not merely local, surface temperatures decrease.

Keywords: climate change, latent heat, evapotranspiration, Bowen ratio, evaporative cooling
S Online supplementary data available from stacks.iop.org/ERL/6/034032/mmedia

1. Introduction

Fluxes of latent heat from the surface to the atmosphere (i.e., predominately evaporative fluxes) are an integral part of the climate system, linking the surface energy balance to the hydrological cycle. Latent heat fluxes have been changed profoundly by human activity, e.g. by anthropogenic climate change (Jung *et al* 2010) and, more importantly, by changes in land use and land cover, in particular deforestation. Latent heat fluxes are usually larger over forests than short vegetation due to deeper rooting, greater transpiring leaf area, and increased roughness (e.g. Pielke 1998). Therefore, forests usually have a lower Bowen ratio than grasslands (i.e. forests have a greater latent heat flux relative to sensible heat flux). Irrigation of crops can also lead to areas of high latent heat flux relative to sensible heat flux (e.g. Boucher *et al* 2004, Lobell *et al* 2006, 2009). This study focuses on climate effects of replacing sensible heating by latent heating, as might occur when a grassland is converted to forest. It is widely known that increasing latent heating at the expense of sensible heating induces local evaporative cooling. However, water vapor plays

[3] Present address: Heat Island Group, Atmospheric Sciences Department, Lawrence Berkeley National Laboratory, One Cyclotron Road, MS90R2000, Berkeley, CA 94720, USA.

many roles in the climate system and the global climate effects of increased latent heating have not been well characterized.

Model simulations suggest that historical deforestation has reduced the latent heat flux on land on the order of half a watt per meter square (W m^{-2}) averaged over all land (e.g. Zhao *et al* 2001, Brovkin *et al* 2006, Pongratz *et al* 2010) with changes up to about 20 W m^{-2} for specific locations and seasons (Bounoua *et al* 2002, Pitman *et al* 2009).

Studies suggest that a reduction (increase) in latent heat increases (decreases) local surface temperatures due to the loss (gain) of evaporative cooling (Claussen *et al* 2001, DeFries *et al* 2002, e.g. Davin and de Noblet-Ducoudre 2010). Water vapor fluxes transport latent heat from the location where water evaporates to where the water condenses. On the global scale, changes in surface evaporative cooling are largely compensated by changes in condensation of the water vapor in the atmosphere (e.g. Lobell *et al* 2006). Thus, changes in latent heating do not directly affect the global energy balance. Therefore, global temperature changes are caused by changes in atmospheric properties such as water vapor content, clouds, and the vertical temperature profile.

In studies of 'realistic' land use and land cover change, it is often difficult to identify what component of climate change may be attributed to changes in latent and sensible heating. Real changes in surface properties would also affect surface albedo and roughness, and it is generally difficult to partition predicted climate change among these causes (Davin and de Noblet-Ducoudre 2010). For example, forests often have lower albedo than croplands, thus more solar radiation is absorbed by forests, which would tend to increase both sensible and latent heat fluxes.

To study climate impacts of latent versus sensible heating, we investigate the climatic effect of changes in the partitioning of latent and sensible heat flux in an idealized scenario by directly forcing the climate system with sources or sinks of latent and sensible heat. We investigate 'forcing response' and subsequent 'temperature response' changes in water vapor, clouds, temperatures, top-of-atmosphere (TOA) energy balance, and feedback parameters. As demonstrated by Gregory *et al* (2004), the climate system adjusts rapidly to an introduced climate forcing and then continues to change over a longer time period as the global mean temperature adjusts. Following Bala *et al* (2010), Andrews *et al* (2009), and others, we use 'fast response' to refer to the rapid response of the atmosphere to changes in forcing and 'slow response' to refer to the rapid response of the atmosphere to slowly evolving surface temperatures. Our aims are to (1) elucidate the processes by which altering surface latent and sensible heat fluxes can alter global (and not just local) climate, and (2) increase understanding of how individual components (i.e. changes in latent and sensible heating) of land use changes alter climate response.

2. Methods

2.1. Model description

The model used in this study is the NCAR Community Atmosphere Model (CAM3.1) (Collins *et al* 2004) coupled to the Community Land Model (CLM3.0) (Oleson *et al* 2004) and a slab ocean model. The configuration used in this study has a finite-volume dynamical core and 2° × 2.5° (longitude × latitude) grid resolution. CAM3.1 has 26 horizontal layers. All simulations were run with a prescribed atmospheric CO_2 concentration of 390 ppm, which is the approximate current level.

2.2. Simulations

To investigate the effect of changes in surface latent and sensible heat fluxes on climate, we performed four simulations. The first was a control simulation with a CO_2 concentration of 390 ppm (referred to as control). The second simulation (referred to as ↑L↓S, more latent and less sensible heating) has an additional 1 W m^{-2} latent heat source applied globally at the interface between the surface and the atmosphere, and a sink of 1 W m^{-2} sensible heat also applied at the interface between the surface and the atmosphere. Thus, surface latent and sensible heat fluxes are repartitioned to favor latent heat fluxes (e.g. decreased Bowen ratio) in an energy neutral way. (Note that while this simulation is balanced in terms of energy, the latent heat sources represent an addition of water, which is balanced by increased precipitation.) Next, to help analyze the separate effects of increased latent and decreased sensible heating, we performed two additional simulations: one (referred to as ↑L for 'more latent') with a 1 W m^{-2} source of latent heat of over the entire Earth surface, and another (referred to as ↓S for 'less sensible') with a 1 W m^{-2} sink of sensible heat fluxes of over the entire Earth surface. In this letter we refer to the aforementioned sources and sinks of latent and sensible heat as 'applied forcings.' The applied forcings investigated herein can be thought of as qualitatively similar to 'ghost forcings' as defined by Hansen *et al* (1997).

In practice, the applied forcings were implemented by adding the heat source and sink terms to the model code subroutine responsible for passing surface fluxes to the model atmosphere (i.e. physpkg.F90 in this model). At each model time step we added the heat source or sink. For example, for ↓S we added to the code, $\mathrm{shf}[i,k] = \mathrm{shf}[i,k] - 1$, where $\mathrm{shf}[i,k]$ is the surface heat flux at time step i and grid cell k in units of W m^{-2}.

2.3. Data analysis

2.3.1. Simulating stationary climates. For each case (i.e. control, ↑L↓S, ↑L, and ↓S), we performed an ensemble of three 20-year simulations and then let one ensemble member of each case run for 100 model years. The global climate model used approaches stationarity within 30 years; 'total responses' are reported for means of the last 70 years of the 100-year simulations, representing a near-stationary climate state. Previous studies often refer to 'total response' as defined in this paper as a change in 'equilibrium' values. Uncertainty is reported as the standard error of annual means ($n = 70$) using the Student-t test with 95% confidence interval (CI) and corrected for temporal autocorrelation (Zwiers and Vonstorch 1995).

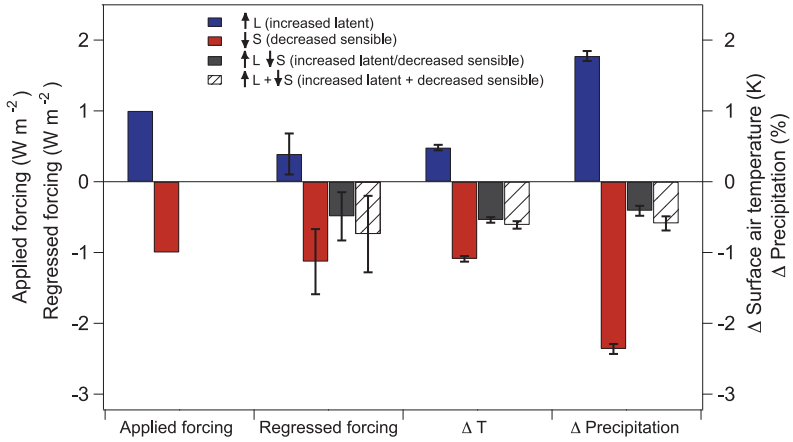

Figure 1. Dependence of surface air temperature, precipitation, and regressed forcing (discussed in section 3.4) on changes in surface latent and sensible heating (applied forcings). All values indicate global average changes relative to the control simulation. ↑L adds a 1 W m^{-2} source of latent heat over the entire Earth surface, and ↓S a 1 W m^{-2} sink of sensible heat fluxes over the entire Earth surface. ↑L↓S includes both the latent source and sensible sink and thus surface latent and sensible heat fluxes are repartitioned to favor latent heat fluxes (e.g. decreased Bowen ratio) in an energy neutral way. ↑L + ↓S is the sum of the ↑L and ↓S simulations. Uncertainty is given by the standard error computed from 70 annual means using the Student *t*-test with 95% confidence interval. The standard error is corrected for autocorrelation (Zwiers and Vonstorch 1995). Numerical values are in supplementary table S1 (available at stacks.iop.org/ERL/6/034032/mmedia).

2.3.2. 'Fast' and 'slow' climate response. In addition to total responses of the climate system, we analyze the fast and slow responses to applied latent and sensible heat forcings. 'Fast response' refers to changes in the climate system that occur as a result of atmospheric adjustment to changes in forcing factors, before longer time scale changes in global and annual-average temperature occur (e.g. Andrews *et al* 2009, Bala *et al* 2010). 'Slow response' refers to changes in the climate system that occur as a result of atmospheric adjustment to changes in surface temperature. For a change in forcing, there is a fast response of the climate system resulting in a top-of-atmosphere energy imbalance. This imbalance can be considered a radiative forcing to be compensated for by changes in top-of-atmosphere fluxes brought about by changes in surface temperature. Thus, the fast response is an indicator for drivers of climate change and the slow response is an indicator of the system response to these drivers (e.g. Gregory *et al* 2004, Bala *et al* 2010).

In this study we calculate the fast and slow responses using the regression method of Gregory *et al* (2004). In this method, changes in global- and annual-mean climate variables of interest are regressed versus changes in global- and annual-mean surface air temperatures, where changes are relative to the control simulation. The fast response is taken to be the *y*-intercept of the regression. In this analysis, fast and slow responses are considered to be independent and additive; thus, the slow response is obtained by taking the total response (see section 2.3.1) minus the fast response (Bala *et al* 2010) (i.e., the total response is the sum of the fast response and the slow response). Regressions for each case (i.e. control, ↑L↓S, ↑L, and ↓S) were computed from annual averages of the ensemble mean of the three 20-year simulations. (Ensembles were used to decrease uncertainty in regression results.)

2.3.3. Sign conventions. In this letter, we report all energy fluxes as positive upward such that the ↑L simulation has positive changes in upward energy flux and ↓S has negative changes in upward energy flux. This convention is more intuitive in this study than the standard positive downward convention because the ↑L simulation is adding a surface latent heat source (i.e. a positive applied forcing) and ↓S a surface sensible heat sink (i.e. a negative applied forcing). The exception to this convention is that cloud forcings are reported as positive downward such that positive cloud forcings indicate additions of energy to the climate system.

3. Results and discussion

3.1. Repartitioning the surface energy balance: ↑L↓S simulation (latent heat source and sensible heat sink)

Changes in surface air temperature and precipitation from the ↑L↓S simulation are shown in figure 1; values are total responses representing 70-year means once the climate has reached a near-stationary state (see supplementary table S1 available at stacks.iop.org/ERL/6/034032/mmedia for numerical values). Note that there is no net addition of energy in the ↑L↓S simulation since we are adding latent heat flux but subtracting an equivalent amount of sensible heat flux, yet climate changes occur. Global mean surface air temperature decreases by 0.54 ± 0.04 K (±95% confidence interval). Precipitation decreases by 0.41 ± 0.07%. In addition, changes in the partitioning of top-of-atmosphere (TOA) radiative fluxes occur; net shortwave radiation (upward positive) increases by 1.0 ± 0.1 W m^{-2} and upward longwave radiation decreases by 1.0 ± 0.1 W m^{-2} (table S1 available at stacks.iop.org/ERL/6/034032/mmedia). Because the applied forcing is energy neutral in the ↑L↓S simulation, the reduction in surface

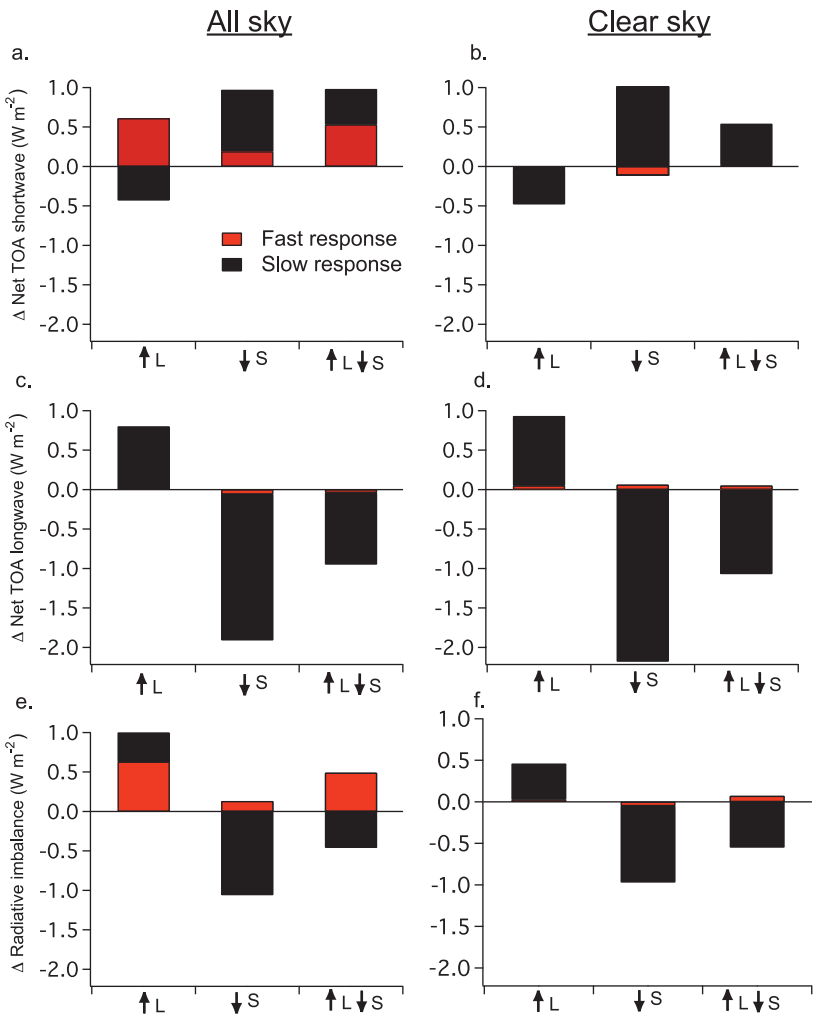

Figure 2. Fast versus slow climate response of radiative variables at the top of atmosphere. Radiative fluxes are positive upward. Fast response refers to changes in the climate system that occur before longer time scale changes in global and annual-average temperature. In this study we calculate the fast climate response using the regression method of Gregory *et al* (2004). Note that values for slow response are not normalized by changes in surface air temperature as it is often presented so that (fast response + slow response) = (total climate response). Numerical values are in supplementary table S2 (available at stacks.iop.org/ERL/6/034032/mmedia).

air temperatures occur as feedbacks including (i) changes in clouds at different altitudes, (ii) changes in atmospheric water vapor, (iii) changes in the vertical temperature profile, and (iv) changes in surface albedo via changes in snow and sea ice. Changes in TOA longwave radiation can occur via (i) (from high clouds), (ii), and (iii), but changes in shortwave radiation occur mostly via (i) (from low clouds) and (iv). These feedbacks can occur either as fast or slow responses of components of the climate system.

3.1.1. Fast versus slow response for ↑L↓S. To help understand the mechanisms by which climate changes occur from repartitioning surface energy, we separate the fast versus slow responses as shown in figures 2 and 3 (see supplementary table S2 available at stacks.iop.org/ERL/6/034032/mmedia for numerical values). The fast response of the TOA radiative imbalance in the ↑L↓S simulation is 0.49 ± 0.34 W m^{-2} (positive upward), exerting a net cooling influence on climate. Note that 'regressed radiative forcing' is defined to be the negative of this value (i.e., positive is a warming influence) (Gregory *et al* 2004).

To analyze mechanisms by which a change in the Bowen ratio can affect the global energy balance, we computed the fast response of various factors to the change in surface energy fluxes (i.e., the response of the factors prior to adjustment of surface temperatures). The radiative imbalance is caused mostly by the increase in low cloud fraction. A rapid increase in low clouds (figure 3) causes a fast response in TOA shortwave cloud forcing of -0.50 ± 0.33 (downward positive), nearly identical to the 'all-sky' fast response in net shortwave radiation of 0.53 ± 0.35 W m^{-2} (upward positive) (figure 2, table S2 available at stacks.iop.org/ERL/6/034032/mmedia). Also note that the change in shortwave radiation of 'cloud free' areas is nearly zero, further implicating that cloud interactions with shortwave radiation is the cause of the fast response in

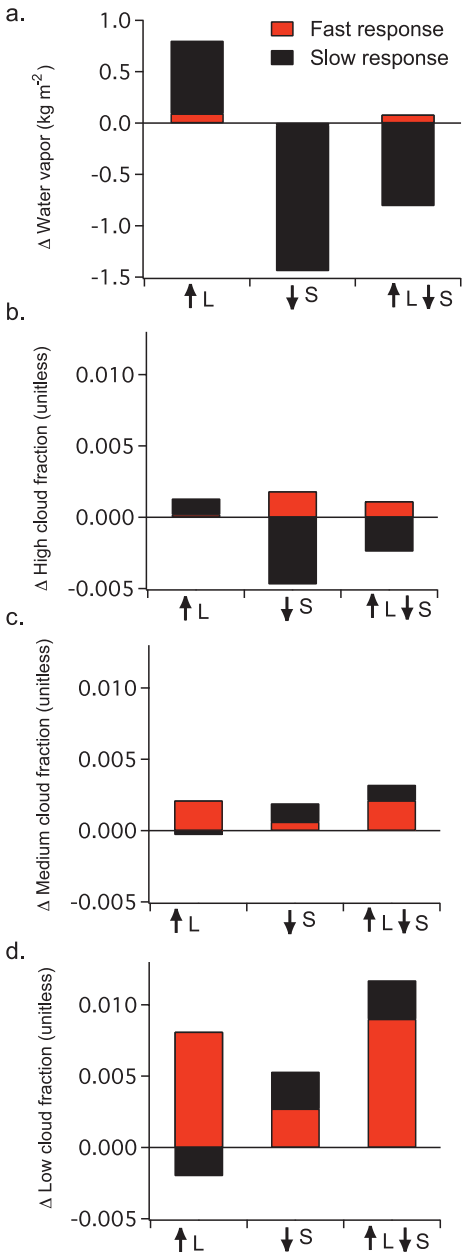

Figure 3. Fast versus slow climate response of water vapor and cloud fractions. Changes in atmospheric water vapor and medium and high clouds occur mostly as slow response feedbacks. There is a significant fast response increase in low clouds, which leads to subsequent slow response changes in climate. Numerical values are in supplementary table S2 (available at stacks.iop.org/ERL/6/034032/mmedia).

TOA fluxes (figure 2). The net response in low clouds and shortwave cloud forcing come primarily from the fast response (figure 3, table S2 available at stacks.iop.org/ERL/6/034032/mmedia).

The fast response change in longwave radiation is nearly zero (figure 2). This suggests that fast responses in atmospheric water vapor and changes in the vertical temperature profile are not driving climate response. The total response in longwave radiation at the TOA (figure 2), as well as changes in atmospheric water vapor (figure 3), are from slow response changes in climate as global temperatures decrease. Fast and slow responses of longwave cloud forcing are nearly zero (table S2 available at stacks.iop.org/ERL/6/034032/mmedia).

3.2. Understanding ↑L↓S in terms of ↑L and ↓S

In an effort to understand the individual effects of the latent heat source and sensible heat sink in ↑L↓S, we now present the results of ↑L and ↓S.

3.2.1. ↑L (latent heat source) simulation. Increasing the upward latent heat flux from the land surface to the atmosphere by 1 W m^{-2} leads to a globally averaged total surface temperature response of $+0.48 \pm 0.04$ K (figure 1, table S1 available at stacks.iop.org/ERL/6/034032/mmedia). This temperature increase is qualitatively consistent with the forcing on the climate system with 1 W m^{-2} of latent heat (i.e. unlike ↑L↓S in which surface energy is repartitioned in an energy neutral way, ↑*L* adds a source of heat to the climate system, which leads to warming). There is a residual change in energy imbalance of 1 W m^{-2} at the top of atmosphere when the climate state is stationary due to this addition of 1 W m^{-2} of latent heat. Increasing upward latent heat flux from the land surface to atmosphere leads to a precipitation increase of $1.77 \pm 0.07\%$.

At the top of atmosphere, the increase in latent heat is redistributed as an increase in net shortwave radiation of 0.2 ± 0.1 W m^{-2} (upward positive), and an increase in upward longwave radiation of 0.80 ± 0.06 (table S1 available at stacks.iop.org/ERL/6/034032/mmedia). The increase in upward shortwave radiation stems from an increase in low cloud fraction of 0.006 ± 0.001, which causes a shortwave cloud forcing of -0.7 ± 0.1 W m^{-2} (positive downward).

3.2.1a. Fast versus slow climate response for ↑L (latent heat source). The fast response of top-of-atmosphere radiation and cloud variables to increasing the upward surface latent heat flux is qualitatively similar to the ↑L↓S simulation (figures 2 and 3, table S2 available at stacks.iop.org/ERL/6/034032/mmedia). The similarity in values between ↑L and ↑L↓S for the fast response of top-of-atmosphere radiative fluxes, changes in cloud fractions, and cloud forcing, indicate that the latent heat component of ↑L↓S is primarily responsible for the fast climate response seen in the ↑L↓S simulation; this suggests that the increase in low clouds and thus reflected solar radiation observed in the ↑L↓S simulation comes primarily from the increase in latent heat flux.

Similar to the ↑L↓S simulation, there is a negligible fast response for top-of-atmosphere longwave radiation (figure 2), suggesting that changes in atmospheric water vapor, vertical temperature profiles, and high clouds change primarily with the slow response associated with temperature change.

3.2.2. ↓S (sensible heat sink) simulation. Decreasing the upward sensible heat flux from the surface to the atmosphere by 1 W m^{-2} leads to a globally averaged total surface temperature response of -1.09 ± 0.04 K (figure 1, table S1

Table 1. Applied forcing, regressed TOA radiative imbalance, regressed forcing, temperature response, feedback parameter to applied forcing, and feedback parameter to regressed forcing. Uncertainty estimates indicate standard errors using the Student-*t* test with 95% confidence interval.

Simulation	Applied forcing (W m^{-2})[a]	Regressed TOA radiative imbalance (W m^{-2})[a,b]	Regressed forcing (W m^{-2})[c]	Total surface air temperature response (K)[d]	Feedback parameter to applied forcing (W m^{-2}) K^{-1} [e]	Feedback parameter to regressed forcing (W m^{-2}) K^{-1} [f]
↑L↓S	0	0.49 ± 0.34	-0.49 ± 0.34	-0.54 ± 0.04	0 ± 0	0.91 ± 0.63
↑L	1	0.61 ± 0.29	0.39 ± 0.29	0.48 ± 0.04	2.1 ± 0.17	0.81 ± 0.61
↓S	−1	0.13 ± 0.46	-1.13 ± 0.46	-1.09 ± 0.04	0.92 ± 0.03	1.0 ± 0.42

[a] Defined as positive upward.
[b] Calculated using the regression method of Gregory *et al* (2004). This is equivalent to the fast response TOA imbalance shown in figure 2.
[c] Calculated as (regressed forcing) = (applied forcing) − (regressed TOA radiative imbalance).
[d] Also known as change in 'equilibrium' surface air temperature.
[e] Defined as (applied forcing)/(total surface air temperature response).
[f] Defined as (regressed forcing)/(total surface air temperature response).

available at stacks.iop.org/ERL/6/034032/mmedia). Again, there is a residual change in energy imbalance of 1 W m^{-2} at the top of atmosphere when the climate state is stationary. Decreasing upward sensible heat flux from the surface to the atmosphere decreases precipitation by $2.36 \pm 0.07\%$.

At the top of atmosphere, the decrease in sensible heat is redistributed as an increase in net shortwave radiation of 0.97 ± 0.08 W m^{-2} (upward positive), and a decrease in upward longwave radiation of 1.91 ± 0.07 (table S1 available at stacks.iop.org/ERL/6/034032/mmedia).

3.2.2a. Fast versus slow response of ↓S (sensible heat sink). The fast responses of top-of-atmosphere shortwave radiation and cloud variables to decreasing upward sensible heat in the ↓S simulation is markedly smaller than those observed in the ↑L↓S and ↑L simulations (figure 2, table S2 available at stacks.iop.org/ERL/6/034032/mmedia). There is a small statistically insignificant decrease in net shortwave radiation at the TOA (figure 2, table S2 available at stacks.iop.org/ERL/6/034032/mmedia) and a small statistically significant increase in low cloud fraction (figure 3, table S2 available at stacks.iop.org/ERL/6/034032/mmedia). This further suggests that the fast climate response observed in the ↑L↓S simulation is due primarily to the addition of latent heat, and not the removal of sensible heat.

Similar to both the ↑L and ↑L↓S simulations, there is a negligible fast response for top-of-atmosphere longwave radiation (figure 2).

3.3. Linearity of ↑L↓S

The linearity of changes in latent and sensible heat fluxes can be assessed by comparing results from the ↑L↓S simulation with the summation of results from the ↑L and ↓S simulations (i.e. ↑L + ↓S in figure 1). Changes in surface air temperature are roughly additive (figure 1) and not statistically distinguishable; summing the ↑L and ↓S simulations suggests a decrease in surface air temperature of 0.61 ± 0.06 K, compared to the decrease in surface air temperature of 0.54 ± 0.04 K from the ↑L↓S simulation. Changes in precipitation are also roughly additive (figure 1) and not statistically distinguishable; summing the ↑L and ↓S simulations suggests a decrease in precipitation of 0.59 ± 0.09%, compared to the decrease in precipitation of 0.41 ± 0.07% from the ↑L↓S simulation.

3.4. Feedback parameters for ↑L, ↓S, and ↑L↓S

The feedback parameters to the imposed latent and sensible forcings are shown in table 1 for each simulation. We define the 'feedback parameter to applied forcing' as the magnitude of the applied forcing (table 1) divided by the total surface air temperature response. These feedback parameters differ among the simulations. Note that this feedback parameter is zero for the ↑L↓S simulation since the applied forcings of latent and sensible heat balance.

Table 1 (and figure 1) also shows values for regressed forcing, defined to be the applied forcing minus the regressed radiative imbalance at the TOA (both positive upward). This regressed forcing parameter represents the total forcing on the climate system since the applied forcing is positive for additions of heat in the climate system and the regressed radiative TOA imbalance is positive upward. (Quantification of the regressed forcing on the climate system needs to include both the radiative imbalance at the boundary (TOA) and any heat sources or sinks, i.e. the latent (sensible) heat source (sink).) We can then define another feedback parameter, which we call the 'feedback parameter to regressed forcing,' as regressed forcing divided by the total surface air temperature response. The feedback parameters to regressed forcing are not statistically distinguishable among the simulations. This supports the hypothesis that the primary explanation for differences in the climate response to different forcing factors are to be found in the fast response to these factors with slow responses showing less sensitivity to differences in forcing characteristics (Andrews *et al* 2009, Bala *et al* 2010). In addition, regressions of TOA radiative imbalance versus temperature response (supplementary figure S1 available at stacks.iop.org/ERL/6/034032/mmedia) show similar slopes, providing further evidence of the similarity in slow climate response among the simulations.

4. Summary

Changes in land cover alter the partitioning of latent and sensible heat fluxes. Surface latent heat flux increases are

expected from e.g. reforestation (e.g. Anderson *et al* 2011) and/or irrigation (e.g. Boucher *et al* 2004, Lobell *et al* 2006, 2009). Surface latent heat flux decreases are expected from CO_2 induced stomatal closure; increases in atmospheric CO_2 concentrations have been linked to the closing of plant stomata, which reduces rates of plant transpiration (Cao *et al* 2009, Bounoua *et al* 2010, Cao *et al* 2010, Andrews *et al* 2011). While changes in sensible heat fluxes alter direct heating of the lower atmosphere in a straightforward way, the climate effect from changes in latent heat fluxes are more complicated. For example, increasing the surface latent heat flux causes local evaporative cooling. But condensation of this water vapor in the atmosphere balances the change in surface evaporative flux and thus evaporative cooling itself is not expected to cause global climate change on a planetary energy balance basis. However climate changes from the repartitioning of latent and sensible heat can occur from changes in the atmosphere (Pielke *et al* 2007) such as increases in clouds, which can alter shortwave and/or longwave radiative fluxes depending on the clouds' altitude, changes in the vertical temperature profile, and changes in atmospheric water vapor.

It is well known that increased evaporation has a cooling influence locally and a warming influence wherever water condenses; however, the net influence on global mean climate has not been carefully assessed. In this letter, we show that altering the partitioning of surface latent and sensible heat by adding a 1 W m^{-2} source of surface latent heat flux and a 1 W m^{-2} sink of sensible heat (i.e. decreasing the Bowen ratio) leads to statistically significant changes in global mean climate. This occurs despite the fact that the energy content of the climate system is not changed. Our analysis has shown that climate changes are caused predominantly by fast response increases in low clouds, which increases reflection of sunlight. Changes in longwave radiation at the top of atmosphere occur only as slow feedbacks as surface air temperature evolves. Thus, changes in atmospheric water vapor and the vertical temperature profiles (which alter longwave radiation at the TOA) are not thought to be primary factors forcing changes in climate.

Further simulations showed that the fast response for cloud changes occurred mostly because of the increase in latent heat flux, and not the decrease in sensible heat flux. Changes in slow cloud responses are similar for adding upward latent heat flux and decreasing sensible heat flux (figure 3).

Note that the found dependency on clouds may be somewhat model dependent since the climate response depends on the altitude of the cloud increase. Increases in clouds at higher altitudes could both increase the relative importance of the trapping of longwave radiation and decrease the relative importance of sunlight reflection, which could alter the results found here. Further, the heating associated with condensation could alter the longwave radiation at the top of atmosphere more significantly if it occurred at higher altitudes; a previous study showed that adding 'ghost forcings' (heat source terms) at high altitudes increases the efficiency at which longwave radiation escapes to space (Hansen *et al* 1997).

The idealized simulations using a global climate model in this study elucidate fundamental understanding of the climate system. Our aim was to increase understanding of how the individual components of land use changes alter climate response. When increasing upward latent heat fluxes while decreasing sensible heat fluxes, there is an increase in low clouds associated with increased evaporation. The increased reflection of downward solar radiation from these clouds is the dominant factor driving the global cooling found here. Increased atmospheric water vapor and differing lapse rates are found to change only as feedbacks associated with temperature change, while low cloud changes mainly occur as fast tropospheric adjustment to changes in latent heat flux. This idealized study suggests that for every watt per square meter that is transferred from sensible to latent heating, on average, as part of the fast response involving low cloud cover, there is approximately a half watt per square meter (0.49 ± 0.34 W m^{-2}) change in the top-of-atmosphere energy balance (positive upward), driving decreases in global surface air temperatures. This study points to the need for improved understanding between changes at Earth's surface, and how they interact with fluxes at the top of the atmosphere to drive regional and global climate change.

References

Anderson R G *et al* 2011 Biophysical considerations in forestry for climate protection *Front. Ecol. Environ.* **9** 174–82

Andrews T, Doutriaux-Boucher M, Boucher O and Forster P M 2011 A regional and global analysis of carbon dioxide physiological forcing and its impact on climate *Clim. Dyn.* **36** 783–92

Andrews T, Forster P M and Gregory J M 2009 A surface energy perspective on climate change *J. Clim.* **22** 2557–70

Bala G, Caldeira K and Nemani R 2010 Fast versus slow response in climate change: implications for the global hydrological cycle *Clim. Dyn.* **35** 423–34

Boucher O, Myhre G and Myhre A 2004 Direct human influence of irrigation on atmospheric water vapour and climate *Clim. Dyn.* **22** 597–603

Bounoua L, DeFries R, Collatz G, Sellers P and Khan H 2002 Effects of land cover conversion on surface climate *Clim. Change* **52** 29–64

Bounoua L, Hall F G, Sellers P J, Kumar A, Collatz G J, Tucker C J and Imhoff M L 2010 Quantifying the negative feedback of vegetation to greenhouse warming: a modeling approach *Geophys. Res. Lett.* **37** L23701

Brovkin V, Claussen M, Driesschaert E, Fichefet T, Kicklighter D, Loutre M, Matthews H, Ramankutty N, Schaeffer M and Sokolov A 2006 Biogeophysical effects of historical land cover changes simulated by six Earth system models of intermediate complexity *Clim Dyn.* **26** 587–600

Cao L, Bala G, Caldeira K, Nemani R and Ban-Weiss G 2009 Climate response to physiological forcing of carbon dioxide simulated by the coupled Community Atmosphere Model (CAM3.1) and Community Land Model (CLM3.0) *Geophys. Res. Lett.* **36** L10402

Cao L, Bala G, Caldeira K, Nemani R and Ban-Weiss G 2010 Importance of carbon dioxide physiological forcing to future climate change *Proc. Natl Acad. Sci. USA* **107** 9513–8

Claussen M, Brovkin V and Ganopolski A 2001 Biogeophysical versus biogeochemical feedbacks of large scale land cover change *Geophys. Res. Lett.* **28** 1011–4

Collins W D *et al* 2004 Description of the NCAR Community Atmosphere Model (CAM 3.0) *NCAR Technical Note NCAR/TN-464+STR* (Boulder, CO: National Center for Atmospheric Research)

Davin E and de Noblet-Ducoudre N 2010 Climatic impact of global-scale deforestation: radiative versus nonradiative processes *J. Clim.* **23** 97–112

DeFries R, Bounoua L and Collatz G 2002 Human modification of the landscape and surface climate in the next fifty years *Glob. Change Biol.* **8** 438–58

Gregory J M, Ingram W J, Palmer M A, Jones G S, Stott P A, Thorpe R B, Lowe J A, Johns T C and Williams K D 2004 A new method for diagnosing radiative forcing and climate sensitivity *Geophys. Res. Lett.* **31** L03205

Hansen J, Sato M and Ruedy R 1997 Radiative forcing and climate response *J. Geophys. Res. Atmos.* **102** 6831–64

Jung M, Reichstein M, Ciais P, Seneviratne S, Sheffield J, Goulden M, Bonan G, Cescatti A, Chen J and de Jeu R 2010 Recent decline in the global land evapotranspiration trend due to limited moisture supply *Nature* **467** 951–4

Lobell D, Bala G and Duffy P 2006 Biogeophysical impacts of cropland management changes on climate *Geophys. Res. Lett.* **33** L06708

Lobell D, Bala G, Mirin A, Phillips T, Maxwell R and Rotman D 2009 Regional differences in the influence of irrigation on climate *J. Clim.* **22** 2248–55

Oleson K W *et al* 2004 Technical Description of the Community Land Model (CLM) *NCAR Technical Note NCAR/TN-461+STR* (Boulder, CO: National Center for Atmospheric Research)

Pielke R 1998 Interactions between the atmosphere and terrestrial ecosystems: influence on weather and climate *Glob. Change Biol.* **4** 461–75

Pielke R A Sr, Adegoke J, Beltran-Przekurat A, Hiemstra C A, Lin J, Nair U S, Niyogi D and Nobis T E 2007 An overview of regional land-use and land-cover impacts on rainfall *Tellus* B **59** 587–601

Pitman A, de Noblet-Ducoudre N, Cruz F, Davin E, Bonan G, Brovkin V, Claussen M, Delire C, Ganzeveld L and Gayler V 2009 Uncertainties in climate responses to past land cover change: first results from the LUCID intercomparison study *Geophys. Res. Lett.* **36** L14814

Pongratz J, Reick C, Raddatz T and Claussen M 2010 Biogeophysical versus biogeochemical climate response to historical anthropogenic land cover change *Geophys. Res. Lett.* **37** L08702

Zhao M, Pitman A and Chase T 2001 The impact of land cover change on the atmospheric circulation *Clim. Dyn.* **17** 467–77

Zwiers F W and Vonstorch H 1995 Taking serial-correlation into account in tests of the mean *J. Clim.* **8** 336–51